Chaos, Solitons and Fractals 202 (2026) 117592

Contents lists available at ScienceDirect

Chaos, Solitons and Fractals

journal homepage: www.elsevier.com/locate/chaos

Evolution of cooperation among migrating resource-oriented agents under environmental variability

Masaaki Inaba [a],*, Eizo Akiyama [b]

[a] Graduate School of Science and Technology, University of Tsukuba, 1-1-1 Tennodai, Tsukuba, 305-8577, Ibaraki, Japan
[b] Institute of Systems and Information Engineering, University of Tsukuba, 1-1-1 Tennodai, Tsukuba, 305-8577, Ibaraki, Japan

ARTICLE INFO

Dataset link: https://github.com/mas178/Inaba2025-2D

Keywords:
Evolution of cooperation
Game theory
Complex systems
Anthropology
Environmental variability
Migration
Agent-based simulation

ABSTRACT

Cooperation is fundamental to human societies. While several basic theoretical mechanisms underlying its evolution have been established, research addressing more realistic settings remains underdeveloped. Drawing on the hypothesis that intensified environmental fluctuations influenced early behavioral evolution in humans during the Middle Stone Age in Africa, we examine the effects of environmental variability and human mobility on the evolution of cooperation. In our model, the variability is represented by randomly moving resource-rich spots across a two-dimensional space, and the mobility is represented by resource-seeking migration of agents. The agents interact cooperatively or competitively for resources while adopting their behavioral strategies from more successful neighbors. Through extensive simulations of this model, we reveal three key findings: (i) with sufficient agent mobility, even modest environmental variability promotes cooperation, but further variability does not enhance cooperation; (ii) with any level of environmental variability, agent mobility promotes cooperation; and (iii) these effects occur because the joint effect of environmental variability and agent mobility disrupts defector groups in resource-rich areas, forming cooperator groups at those sites. Although previous studies examined environmental variability and mobility separately, to the best of our knowledge, this is the first study to analyze their joint effects on the evolution of cooperation. These findings suggest that environmental variability can promote cooperative group formation without enhanced cognitive abilities, providing new insights into the evolution of human cooperation and, by extension, sociality.

1. Introduction

Cooperative behavior is a fundamental feature of human societies. Yet this widespread behavior poses an evolutionary paradox: while evolutionary theory suggests that individuals act to maximize their own fitness, cooperation appears to favor the benefit of others or groups over that of individuals. Numerous previous studies [1–6] have addressed this puzzle, identifying several theoretical mechanisms that explain the evolution of cooperation. However, several factors that influence cooperation in natural settings, e.g., environmental variability, mobility, complex networks, norms, and memory, remain theoretically underexplored. In this paper, we focus on how environmental variability and agent mobility shape the evolutionary dynamics of cooperation.

Although most theoretical studies on the evolution of cooperation do not explicitly consider environmental factors, several studies have examined these aspects, typically in biological or physical contexts: extrinsic population variability [7,8], variability in game structure [9–11], variability in selection intensity [12], differences in resource pressure [13], and environmental feedback [14,15].

* Corresponding author.
E-mail address: masaaki.inaba@gmail.com (M. Inaba).

https://doi.org/10.1016/j.chaos.2025.117592
Received 16 September 2025; Received in revised form 30 October 2025; Accepted 8 November 2025
Available online 15 November 2025
0960-0779/© 2025 The Authors. Published by Elsevier Ltd. This is an open access article under the CC BY license (http://creativecommons.org/licenses/by/4.0/).

Differing from these studies, which primarily focused on biological and physical contexts, we investigate cooperation under the condition of environmental variability from an anthropological perspective, drawing on the Variability Selection Hypothesis (VSH) [16–19]. The VSH posits that variable and unpredictable environments during the Middle Stone Age (MSA) in Africa were crucial drivers of human evolution. The VSH is based on the temporal correspondence between periods of increased environmental variability and the sophistication of archaeological artifacts, though the underlying causal dynamics are not yet fully resolved. In a previous study [20], we worked to clarify these dynamics by demonstrating that environmental variability can promote cooperation through the interplay between environmental disruptions and social network structures that support cooperation. However, the previous study does not incorporate mobility, which is an essential trait of pre-sedentary human populations in the MSA.

The evolution of cooperation among mobile agents has been studied actively. For example, Dugatkin and Wilson (1991) [21] performed a pioneering study in this area, and Vainstein et al. (2007) [22] subsequently established that mobility promotes cooperation under very minimal assumptions. Recently, various migration strategies [23–29] that differ in terms of the trigger conditions and migration distance have been proposed, and the evolution of cooperation under each strategy has been investigated. However, to the best of our knowledge, research that addresses exogenous environmental variability in the evolution of cooperation with migration has yet to be conducted.

In summary, although previous studies have investigated cooperation under environmental variability and cooperation with mobility, no studies have integrated both factors. Motivated by our interest in environmental variability and human behavioral evolution during the MSA in Africa, this study focuses on how environmental variability and agent mobility jointly affect the evolution of cooperation.

2. Model

In this study, we developed a multiagent simulation model to examine how agent mobility and environmental variability jointly influence the evolution of cooperation in spatially structured populations. Due to the limited availability of archaeological data on spatial resource distributions and hominin behavioral patterns during the MSA, we adopted an abstracted approach that prioritizes the identification of fundamental mechanisms over reproducing specific historical scenarios. This model incorporates four key processes, i.e., (i) environmental variability on a two-dimensional (2D) lattice, (ii) pairwise game interactions, (iii) conditional agent migration driven by resource availability, and (iv) strategy updating. These processes are described in the following subsections.

2.1. Environmental variability

The spatial structure is represented by a 2D lattice with periodic boundary conditions. Here, N agents are distributed randomly across the cells, and each cell contains at most one agent. Each cell maintains a resource level that varies both spatially and temporally. We define a Source of Resources (SoR) as a focal point that generates spatial resource gradients in the environment, and these SoRs serve as simplified representations of the natural foraging areas commonly found near rivers, lakes, and coastlines. Each SoR creates a gradient where resource availability typically decreases with increasing distance from the SoR. In addition, multiple SoRs may coexist, thereby forming overlapping zones of resource abundance.

In this model, each agent accumulates resources (represented by the agent's fitness value) through interactions, and local prosperity is defined by a resource threshold $\theta_{x,y}$ for each cell (x, y), where $0 \leq \theta_{x,y} \leq 1$. Agents with fitness values that are less than the threshold $\theta_{x,y}$ are more likely to migrate and update their strategies, and agents with fitness values greater than the threshold remain unchanged. Therefore, locations with lower thresholds impose less pressure for behavioral change, indicating that these locations are prosperous and rich in resources. Here, the threshold $\theta_{x,y}$ is determined by the cumulative influence of all SoRs and is calculated as follows:

$$\theta_{x,y} = \frac{D_{x,y} - D_{\min}}{D_{\max} - D_{\min}}, \quad D_{x,y} = \sum_{i=1}^{n} d_{x,y}^{(i)} \tag{1}$$

where $d_{x,y}^{(i)}$ denotes the Euclidean distance from cell (x, y) to the ith SoR, calculated under periodic boundary conditions, and $D_{\min}$ and $D_{\max}$ denote the minimum and maximum values of $D_{x,y}$ across the entire grid, respectively.

We examine two spatial configurations, which we refer to as 1-SoR and 2-SoR. In the 1-SoR configuration (a 200×200 grid), a single SoR generates a concentric resource gradient, capturing the essential geographical pattern of an oasis-like environment (Fig. 1a). In the 2-SoR configuration (a 400×200 grid), two SoRs generate a corridor of resource gradient, capturing the essential geographical pattern of riverine or coastal environments where resources are distributed along a line (Fig. 1b).

Environmental variability is modeled through the stochastic movement of SoRs, reflecting the unpredictable nature of the landscape dynamics observed during the MSA in Africa. Each SoR moves to a randomly selected adjacent cell within the Moore neighborhood with a probability p_{EV} $(0 \leq p_{EV} \leq 1)$ at each time step, and the direction is selected uniformly at random from the eight neighboring cells. In this process, the parameter p_{EV} governs the intensity of the environmental variability, where $p_{EV} = 0$ corresponds to a static environment, and higher p_{EV} values represent more intense environmental variability.

Throughout this study, the neighborhood is defined as the Moore neighborhood (i.e., eight neighboring cells). This choice better approximates the continuous spatial movement of SoRs and mobile agents than the von Neumann neighborhood (i.e., four orthogonal cells), where movement is restricted to only cardinal directions. In addition, for distance calculations, particularly when determining resource gradients from SoRs, the Euclidean distance is employed to produce smooth, circular gradients that better represent natural resource distributions than other metrics, e.g., the Manhattan or Chebyshev distances.

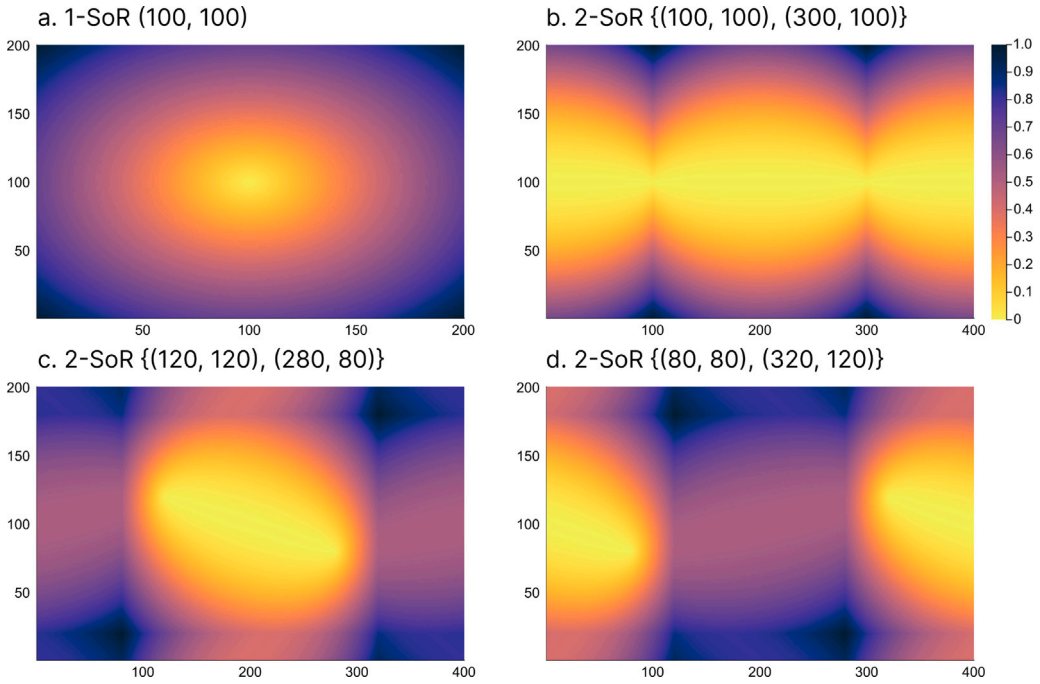

Fig. 1. Spatially heterogeneous prosperity patterns generated by SoR(s). The colors indicate the resource threshold $\theta_{x,y}$. (a) A single SoR located at $(100, 100)$ on a 200×200 grid generates a concentric resource gradient. (b) Two SoRs located at $(100, 100)$ and $(300, 100)$ on a 400×200 grid generate a band-shaped resource gradient. (c) and (d) Examples of the stochastic movement of SoRs that dynamically reshapes the resource landscapes.

2.2. Game

Games represent cooperative or competitive interactions between agents that involve the gain or loss of resources. Each agent holds a strategy, either cooperation (C) or defection (D), which determines its behavior in interactions. In every time step, each agent plays pairwise games with all its neighbors and accumulates a payoff π_j, which is then converted into fitness ω_j ($j \in [1, \dots, N]$, $0 < \omega_j < 1$), representing the agent's resource level.

The payoff matrix of the game is defined as follows:

	C	D
C	R	S
D	T	P

(2)

where $R = 1$, $0 < T < 2$, $-1 < S < 1$, and $P = 0$. To ensure the robustness of the results across a range of social dilemma contexts, we consider various game structures, including the Prisoner's Dilemma ($T > R > P > S$), Stag Hunt ($R > T > P > S$), and Snowdrift ($T > R > S > P$) games.

The accumulated payoff π_j is transformed into the fitness ω_j using a sigmoid function as follows:

$$\omega_j = \frac{1}{1 + \exp(-k(\pi_j - \pi_0))} \tag{3}$$

where k determines the steepness of the sigmoid curve, and π_0 sets the baseline payoff at which $\omega_j = 0.5$. Here, we set $k = 1$ for moderate sensitivity and set $\pi_0 = 4.0$ to center the sigmoid around common payoff values found in mixed-strategy populations. Given that each agent can accumulate payoffs from up to eight of its neighbors, the theoretical payoff range is $8S$ to $8R$ and $8P$ to $8T$ for cooperators and defectors, respectively. With our parameter constraints, this yields a payoff range of $-8 < \pi_j < 16$.

2.3. Migration

At each time step, agents migrate if their fitness ω_j is less than the resource threshold $\theta_{x,y}$ at their current location. Any agent that meets this condition migrates with probability p_M and remains at the location with the complementary probability $1 - p_M$. The migration direction follows a resource-oriented bias, where an agent moves toward a neighboring cell with the lowest $\theta_{x,y}$ value with probability p_{SoR} (SoR orientation) and moves randomly within the neighborhood with the complementary probability $1 - p_{SoR}$. Cells occupied by other agents are excluded from the candidate destinations. The agents migrate asynchronously in a randomized order to avoid movement conflicts.

Table 1
Model parameters used in the simulations.

Parameter	Description	Value options
$W \times H$	Grid dimensions	$200 \times 200, 400 \times 200$
N	Total number of agents	$500 \times 2^{\{0,1,2,3,4,5\}}$
ϕ_C^0	Initial frequency of cooperators	$0, 0.5, 1$
n_{SoR}	Total number of SoRs	1, 2
p_{EV}	Probability of SoR shift	0 to 1 (step: 0.1)
R	Payoff for mutual cooperation	1
T	Payoff for defection against cooperator	0 to 2 (step: 0.1)
P	Payoff for mutual defection	0
S	Payoff for cooperation against defector	−1 to 1 (step: 0.1)
p_M	Probability of migration	0 to 1 (step: 0.1)
p_{SoR}	Probability of resource-oriented migration	0 to 1 (step: 0.1)
μ	Probability of mutation	$0, 0.01$

2.4. Strategy update

At each time step, agents update their strategies synchronously if their fitness ω_j is less than the resource threshold $\theta_{x,y}$. Any agent that meets this condition adopts the strategy of the most successful neighbor (i.e., the neighbor with the highest fitness). This process is subject to mutation, where the adopted strategy is replaced by the opposite strategy (e.g., from C to D or vice versa) with probability μ.

We note that asynchronous updating [30,31] is more realistic and the choice of updating protocol can significantly affect outcomes in densely packed models [30]. However, unlike densely connected lattice models where agents interact with many neighbors simultaneously, our agents typically interact with only a few neighbors on each resource patch. This sparsity reduces the interdependence between neighboring strategy updates, making the dynamics largely insensitive to the updating protocol.

2.5. Evaluation

To investigate the effects of environmental variability and agent mobility on the evolution of cooperation, simulations are performed under a range of parameter configurations, as shown in Table 1.

Each configuration is evaluated through 100 independent trials of 10000 generations each. As the primary outcome measure, we compute the cooperation rate ϕ_C, which is defined as the average proportion of agents employing the C strategy during the final 5000 generations averaged over all trials.

3. Results

3.1. Influence of environmental variability and agent mobility

Fig. 2 shows the combined effects of environmental variability (p_{EV}) and agent mobility (p_M) on the cooperation rate ϕ_C. As can be seen, in stable environments ($p_{EV} = 0$) or with low agent mobility ($p_M \lesssim 0.2$), cooperation fails to evolve. In contrast, with sufficient agent mobility ($p_M \gtrsim 0.2$), even modest environmental variability ($p_{EV} = 0.1$) promotes cooperation; however, further variability ($p_{EV} > 0.1$) does not enhance cooperation. In addition, agent mobility promotes cooperation with any level of environmental variability ($p_{EV} > 0$).

Fig. 3 shows the role of environmental variability in the evolution of cooperation. This representative simulation is presented to understand the temporal dynamics underlying the statistical patterns displayed in Fig. 2. Whereas Fig. 2 considers fixed variability levels throughout the simulation, here we apply a cyclic p_{EV} alternating between stable and variable conditions every 2000 generations over a total of 10000 generations. Under these cyclic conditions, cooperation initially increases to slightly less than 50% during the first stable phase and then plateaus, as shown in Fig. 3a. A pronounced increase is observed once the system enters the variable phase, which reinforces the conclusion that environmental variability plays a pivotal role in promoting cooperation.

The observed dynamics can be understood as a three-stage process: (i) the formation of a few large defector groups fixed in resource-rich areas, (ii) their collapse induced by environmental variability, and (iii) subsequent emergence of several small cooperator groups. Figs. 3b–f show snapshots from the simulation presented in Fig. 3a. A full video showing this process is provided in the Supplementary Material. In the first stable phase as shown in Fig. 3b, the agents in prosperous areas have no need to cooperate or move, whereas those in less prosperous areas must cooperate or move to prosperous areas. At the boundaries between these two areas, fixed walls are formed by defectors who do not need to change their strategies or move further. During the next variable phase as shown in Figs. 3c–e, agents located on boundaries are forced to cooperate or move due to the environmental changes, thereby leading to the collapse of the stable defector group as shown in the central area of Fig. 3c. In place of the defector group, the agents form several small cooperator groups to survive even in severe environmental conditions (Fig. 3d). Then, the same process occurs in the areas at both ends of the figure (Figs. 3e and f).

In contrast, cooperation cannot evolve if the agent mobility is insufficient relative to the intensity of the environmental variability (refer to the lower area of Fig. 2), which occurs because excessively rapid SoR movement prevents the formation of both defector structures and small cooperator groups, as shown in Fig. 4. Thus, environmental variability and sufficient agent mobility promote cooperation by preventing fixed defector structures and encouraging the agents to form cooperator groups for survival.

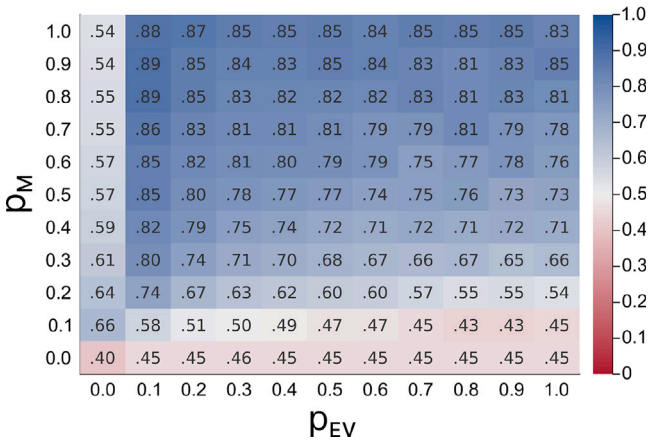

Fig. 2. Influence of environmental variability (p_{EV}) and agent mobility (p_M) on the cooperation rate (ϕ_C). The figure shows that cooperation emerges only when both $p_{EV} \gtrsim 0.1$ and $p_M \gtrsim 0.2$, with neither factor alone being sufficient to promote cooperation. Each cell shows the mean value over 100 independent runs. The results are shown for a representative parameter set ($N = 1000$, $\phi_C^0 = 0.0$, 2-SoR, $T = 1.2$, $S = -0.2$, $p_{SoR} = 0.1$, $\mu = 0.01$). Qualitatively similar patterns are observed for other parameter configurations. The standard deviations across runs are less than 0.15 for all cells.

3.2. Influence of other parameters on cooperation rate

To gain further insights into the findings presented above and assess their robustness, we investigated the effects of additional parameters, including the population size (N), the number of SoRs (n_{SoR}), the initial frequency of cooperators (ϕ_C^0), the SoR orientation (p_{SoR}), the payoff parameters (T, S), and the mutation rate (μ).

3.2.1. Population size

Larger population size promotes cooperation to some extent, as shown in Fig. 5, because the cooperators can more easily find other cooperators when the population size is sufficiently large. Another notable observation is that the cooperation rates for $(p_{EV}, p_M) = (0.0, 0.1)$ (red dashed line) and $(0.1, 0.1)$ (blue dashed line) exhibit a crossover at approximately $N = 2000$. For small populations ($N < 2000$) with low agent mobility, cooperation evolves more readily without environmental variability. In stable environments ($(p_{EV}, p_M) = (0.0, 0.1)$), both the defector and cooperator groups persist once established, although the formation of these groups is slow due to the low agent mobility. In contrast, environmental variability with low agent mobility ($(p_{EV}, p_M) = (0.1, 0.1)$) creates perpetual fluidity that prevents the formation of both structures.

Larger populations alter this relationship. Larger populations increase the encounter rate among cooperators, which allows for the formation of cooperator groups even under environmental variability. In stable environments, the structures remain fixed, thereby limiting the impact of the higher encounter rate. In contrast, the higher encounter rate in fluid environments facilitates group formation. Thus, environmental variability becomes advantageous for cooperation above the critical population size.

A less prominent but similar crossover occurs at approximately $N = 8000$ between $(p_{EV}, p_M) = (0.0, 0.1)$ (red dashed line) and $(p_{EV}, p_M) = (0.0, 1.0)$ (red solid line). This crossover reflects the spatial constraints of the defector groups in stable environments ($p_{EV} = 0$). For $N \lesssim 8000$, high mobility ($p_M = 1.0$) allows more agents to reach the resource-rich areas where cooperation is not required. In contrast, low mobility ($p_M = 0.1$) keeps the agents in peripheral areas where cooperation is required for survival.

However, larger populations ($N \gtrsim 8000$) exhibit three nested zones: central rich areas, where cooperation is not required; surrounding moderate areas, where the agents can survive through cooperation; and the most peripheral harsh areas, where agents cannot survive even with cooperation because the resource threshold exceeds what can be provided through cooperation. Under these conditions, high mobility allows the agents to escape from the harsh areas to the moderate cooperative areas, whereas low mobility traps the agents in the harsh areas. In addition, the central rich areas have already reached their physical capacity due to the large population; thus, further population increases have no effect in these areas. Consequently, the effect of mobility on the cooperation rate (ϕ_C) reverses as the population size increases.

3.2.2. Number of SoRs and initial cooperation rate

Both the number of SoRs (n_{SoR}) and the initial frequency of cooperators (ϕ_C^0) have a significant influence on the results. While the 2-SoR configuration forms large band-shaped defector groups (Fig. 3b), the 1-SoR configuration only forms a small, circular resource-rich area (Fig. 6b). When a large defector group collapses and is replaced by small cooperator groups, as observed with the 2-SoR setting, the impact on the overall system is substantial. In contrast, under the 1-SoR setting, when a small defector group undergoes the same replacement, the effect is less conspicuous than in the 2-SoR setting (Fig. 6a). In terms of ϕ_C^0, initiation with no cooperators ($\phi_C^0 = 0$) in the 2-SoR configuration results in large defector groups, whereas intermediate or full cooperation ($\phi_C^0 = 0.5$

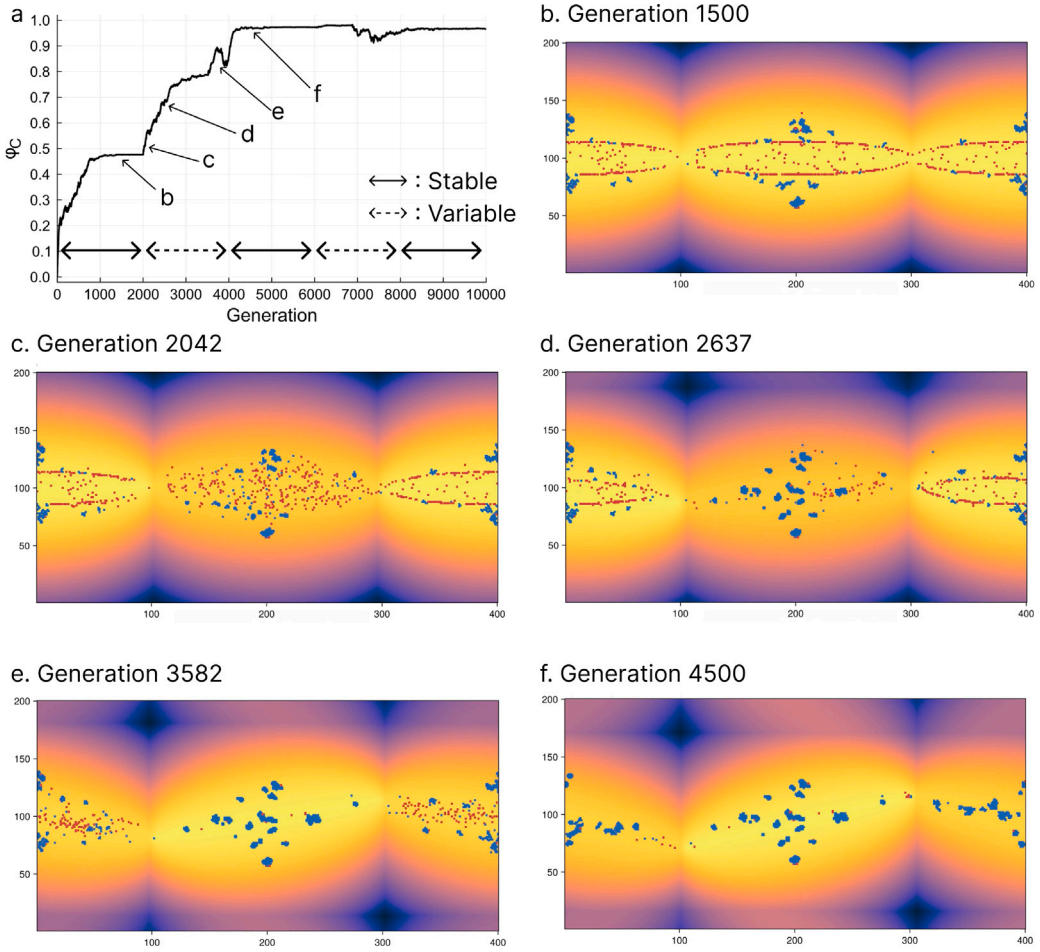

Fig. 3. Temporal dynamics under cyclic environmental variability. The figure demonstrates that environmental variability drives cooperation by disrupting stable defector groups in resource-rich areas and facilitating the formation of multiple small cooperator groups. (a) Cooperation rate over 10000 generations with p_{EV} alternating between stable ($p_{EV} = 0$) and variable ($p_{EV} = 0.1$) phases every 2000 generations. (b)–(f) Spatial snapshots at each generation. Blue and red dots represent cooperators and defectors, respectively. Background colors indicate the resource threshold $\theta_{x,y}$ as in Fig. 1. Parameter settings: $N = 1000$, $\phi_C^0 = 0.0$, 2-SoR, $T = 1.2$, $S = -0.2$, $p_M = 1.0$, $p_{SoR} = 0.1$, $\mu = 0.01$.

or 1) maintains the large structure but with a higher cooperator frequency within it (Fig. 7). Consequently, these conditions mask the significant effects of defector group collapse and cooperator group formation observed in Section 3.1.

We also confirmed that changing the distance metric from Euclidean to the Chebyshev or Manhattan distance alters the size and shape of the groups, thereby affecting the results. However, these effects are primarily attributed to differences in the group size rather than the shape. Thus, comparisons among these distance metrics can be interpreted as theoretically equivalent to the comparison between the 1-SoR and 2-SoR settings. Essentially, the formation of large defector groups in stable environments is the critical prerequisite for the results described in Section 3.1.

3.2.3. SoR orientation

SoR orientation (p_{SoR}) noticeably influences the cooperation rate (Fig. 8). Increasing p_{SoR} from 0 to 0.1 improves cooperation rates by approximately 20%–40% if $p_{EV} > 0$. However, further increases in p_{SoR} beyond 0.2 reduce the cooperation rate. This reduction occurs because excessive p_{SoR} increases the likelihood of agent collisions, which in turn hinders effective migration. These findings suggest that some randomness in the agent mobility is required to maintain a high level of cooperation.

3.2.4. Payoff parameters and mutation rate

We also investigated the effects of varying the values of the payoff parameters (T, S) across several game structures and the mutation rate μ (including $\mu = 0$ and $\mu = 0.01$). While these variations did not yield qualitatively new insights, they confirmed the robustness of the observed patterns. For completeness, the corresponding results are provided in the Supplementary Material.

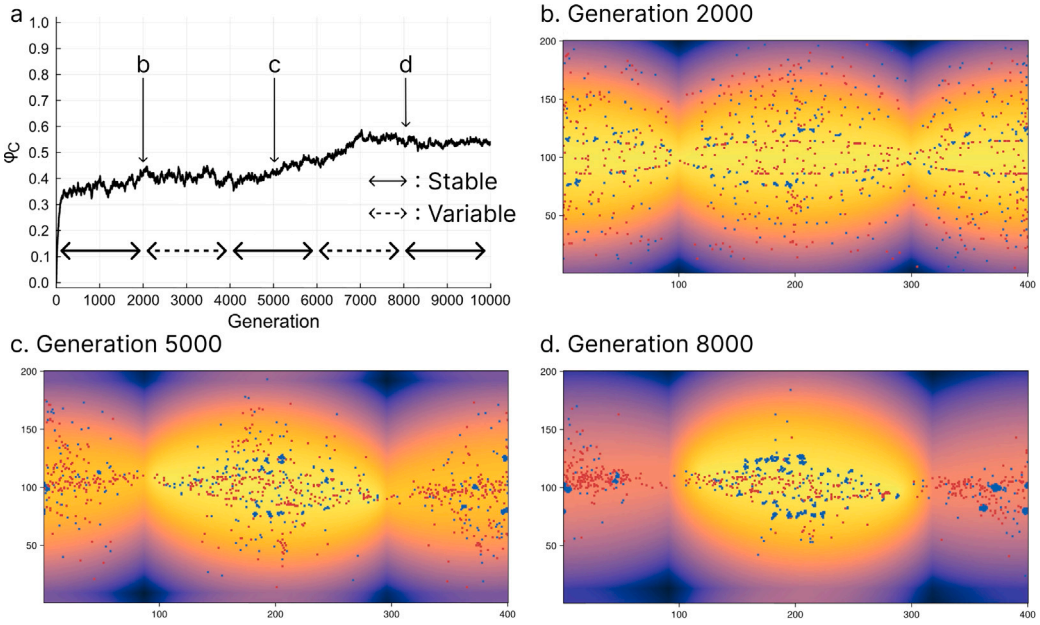

Fig. 4. Temporal dynamics under cyclic environmental variability with low agent mobility. In contrast to Fig. 3 ($p_M = 1.0$), here lower mobility ($p_M = 0.1$) prevents agents from keeping up with the environmental variability. As a result, cooperation fails to evolve. All other parameters and the interpretation of the visual elements are the same as in Fig. 3.

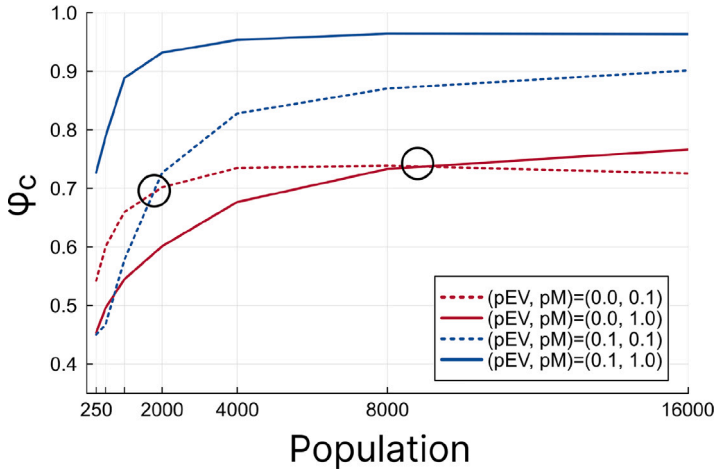

Fig. 5. Influence of population size (N) on cooperation rate (ϕ_C). The figure shows two crossovers: at $N \approx 2000$ between $(p_{EV}, p_M) = (0.0, 0.1)$ (red dashed) and $(0.1, 0.1)$ (blue dashed), and at $N \approx 8000$ between $(0.0, 0.1)$ (red dashed) and $(0.0, 1.0)$ (red solid). These crossovers reflect how population size alters the relative benefits of environmental variability and mobility through changes in cooperator encounter rates and spatial resource distribution. Parameter settings: $\phi_C^0 = 0.0$, 2-SoR, $T = 1.2$, $S = -0.2$, $p_{SoR} = 0.1$, $\mu = 0.01$. The results for $N = 32000$ are omitted because they exhibited negligible differences from $N = 16000$. (For interpretation of the references to color in this figure legend, the reader is referred to the web version of this article.)

4. Discussion

In this study, we examined the joint effects of environmental variability and agent mobility on the evolution of cooperation to understand the causal dynamics of these factors in spatially structured populations. The model incorporates unpredictable environmental variability by implementing SoRs that move randomly across a 2D space, generating dynamic spatial heterogeneity in resource availability. Agents accumulate resources through cooperative or competitive interactions, and the agents with lower resource levels are more likely to migrate to neighboring cells and update their strategies. With this model, we identified three key findings. First, with sufficient agent mobility, even modest environmental variability promotes cooperation; however, further

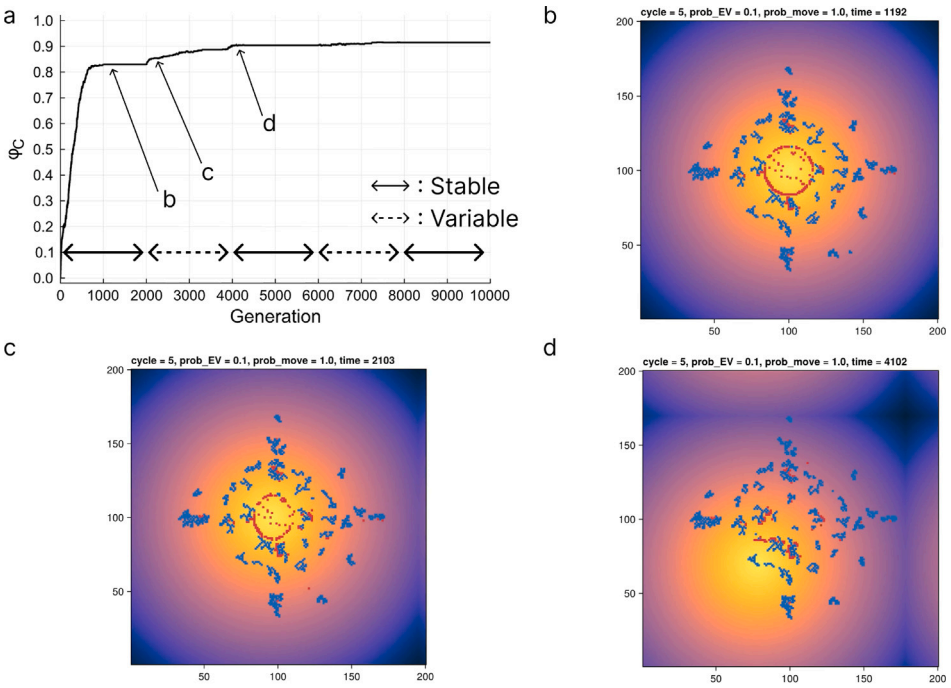

Fig. 6. Temporal dynamics under cyclic environmental variability in the 1-SoR configuration. The figure shows that the 1-SoR configuration forms only a small circular resource-rich area, resulting in a less pronounced impact of defector group collapse on overall cooperation levels compared to Fig. 3 (2-SoR). All other parameters and the interpretation of the visual elements are the same as in Fig. 3.

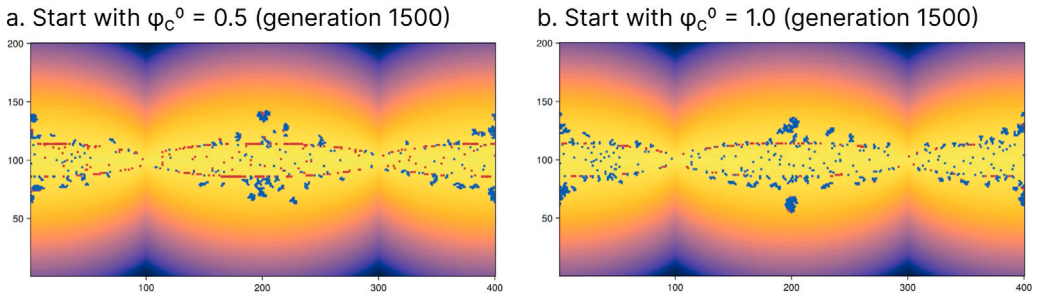

Fig. 7. Central resource-rich areas under $\phi_C^0 = 0.5$ or 1.0. The figure shows that higher initial cooperation rates maintain larger cooperative structures in resource-rich areas, masking the effects of defector group collapse and cooperator group formation observed with $\phi_C^0 = 0.0$. All parameters (except ϕ_C^0) and the interpretation of the visual elements are the same as in Fig. 3.

variability does not enhance cooperation. Second, with any level of environmental variability, agent mobility promotes cooperation. Third, these effects occur because environmental variability disrupts a few large stable defector groups that form in resource-rich areas, and agent mobility effectively enables the formation of numerous small cooperator groups at those sites.

The findings of this study are expected to contribute to our understanding of the evolution of cooperation in several important ways. First, we have discovered the joint impact of environmental variability and agent mobility on cooperation, which previous studies [7–12,22–29] examined independently. Second, in the VSH [16–19], environmental variability has conventionally been understood as a selective pressure on individual cognitive abilities during the MSA in Africa [32–34], implying a pathway from the variability to enhanced intelligence and then to increased sociality. However, we have demonstrated that the variability can also affect sociality directly. Specifically, the agents in our model collectively form cooperative groups in response to environmental variability, even though they simply repeat interactions, migration, and strategy updating without increasing their intelligence. This discovery enhances our understanding of whether intelligence or sociality came first in human evolution and of their complementary coevolution [20,35–38]. Third, our model and the discovered mechanisms are highly general and abstract; thus, they are not limited to the context of the current study. With suitable adaptations, there may be potential for interdisciplinary applications in different fields, e.g., biology, ecology, and understanding modern social phenomena.

Despite these contributions, this study has several limitations that suggest directions for future research.

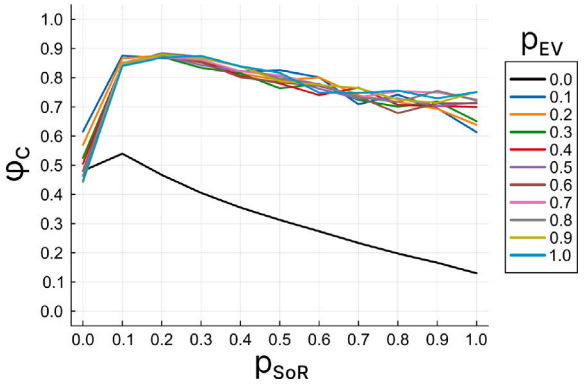

Fig. 8. Influence of SoR orientation (p_{SoR}) on the cooperation rate (ϕ_C). The figure shows that moderate SoR orientation ($p_{SoR} \approx 0.1$) maximally promotes cooperation, while excessive p_{SoR} reduces cooperation due to increased agent collisions that hinder effective migration. Parameter settings: $N = 1000$, $\phi_C^0 = 0.0$, 2-SoR, $p_M = 1.0$, $T = 1.2$, $S = -0.2$, $\mu = 0.01$.

First, the model aims to understand abstract macroscopic phenomena rather than to reproduce or predict specific real-world outcomes; thus, it adopts simplifications at various levels. For example, while our model employs pairwise interactions, multiplayer games such as public goods games [27,29,31,39,40] have been extensively studied. Regarding strategy updating, strategy sets beyond All-C and All-D [21] could be considered. Additionally, while our model employs social learning where agents update strategies by imitating others, individual learning mechanisms could also be explored. For instance, agents could balance individual and social learning based on environmental uncertainty [41], develop context-dependent learning propensities influenced by social dominance [42], or adaptively adjust their strategies through reinforcement learning algorithms [43]. As for migration, our model considers only resource levels as the trigger for migration. However, it is known that migration costs [44] and social relationships between agents [23,28] are also important factors that determine collective dynamics. Future research can address these simplifications and limitations by investigating these scenarios.

Second, this study will ultimately require a more formal mathematical foundation. As is typical of multiagent approaches, our model–though much simpler than the real world–remains overly complex for analytical treatment. Thus, we need to explore prospects for mathematical formalization by reproducing the key aspects of the results using simpler models.

Third, this study primarily relies on general patterns described in the VSH rather than empirical data from the MSA in Africa. This limitation is common to theoretical studies on the evolution of cooperation. This is because evidence from this ancient period is sparse, and more fundamentally, cooperative behaviors cannot be directly preserved in archaeological remains, leaving only indirect evidence. Although these constraints are fundamental, we hope that theoretical studies such as ours will play a crucial role in directing empirical research and providing frameworks to interpret empirical findings.

CRediT authorship contribution statement

Masaaki Inaba: Writing – review & editing, Writing – original draft, Visualization, Validation, Software, Resources, Project administration, Methodology, Investigation, Formal analysis, Conceptualization. **Eizo Akiyama:** Writing – review & editing, Supervision.

Declaration of Generative AI and AI-assisted technologies in the writing process

During the preparation of this work, the authors used ChatGPT (OpenAI) and Claude (Anthropic) in order to improve the language and clarity of the manuscript. After using these tools, the authors reviewed and edited the content as needed and take full responsibility for the content of the publication.

Declaration of competing interest

The authors declare that they have no known competing financial interests or personal relationships that could have appeared to influence the work reported in this paper.

Acknowledgments

This work was supported by JSPS KAKENHI Grant Number JP23K20588 and by the Fujikura Foundation, Japan.

Appendix A. Supplementary data

Supplementary material related to this article can be found online at https://doi.org/10.1016/j.chaos.2025.117592.

Data availability

All data, as well as the code required to run the simulations and generate the figures, are available at https://github.com/mas178/Inaba2025-2D.

References

[1] Nowak MA. Five rules for the evolution of cooperation. Science 2006;314(5805):1560–3. http://dx.doi.org/10.1126/science.1133755.
[2] West SA, Griffin AS, Gardner A. Evolutionary explanations for cooperation. Curr Biol 2007;17(16):R661–72. http://dx.doi.org/10.1016/j.cub.2007.06.004.
[3] Perc M, Szolnoki A. Coevolutionary games–a mini review. Biosystems 2010;99(2):109–25. http://dx.doi.org/10.1016/j.biosystems.2009.10.003.
[4] Rand DG, Nowak MA. Human cooperation. Trends Cogn Sci 2013;17(8):413–25. http://dx.doi.org/10.1016/j.tics.2013.06.003.
[5] Perc M, Jordan JJ, Rand DG, Wang Z, Boccaletti S, Szolnoki A. Statistical physics of human cooperation. Phys Rep 2017;687:1–51. http://dx.doi.org/10.1016/j.physrep.2017.05.004.
[6] West SA, Cooper GA, Ghoul MB, Griffin AS. Ten recent insights for our understanding of cooperation. Nat Ecol Evol 2021;5(4):419–30. http://dx.doi.org/10.1038/s41559-020-01384-x.
[7] Brockhurst MA, Buckling A, Gardner A. Cooperation peaks at intermediate disturbance. Curr Biol 2007;17(9):761–5. http://dx.doi.org/10.1016/j.cub.2007.02.057.
[8] Miller S, Knowles J. Population fluctuation promotes cooperation in networks. Sci Rep 2015;5:11054. http://dx.doi.org/10.1038/srep11054.
[9] Gokhale CS, Hauert C. Eco-evolutionary dynamics of social dilemmas. Theor Popul Biol 2016;111:28–42. http://dx.doi.org/10.1016/j.tpb.2016.05.005.
[10] Stojkoski V, Karbevski M, Utkovski Z, Basnarkov L, Kocarev L. Evolution of cooperation in networked heterogeneous fluctuating environments. Phys A 2021;572:125904. http://dx.doi.org/10.1016/j.physa.2021.125904.
[11] Kroumi D, Martin É, Li C, Lessard S. Effect of variability in payoffs on conditions for the evolution of cooperation in a small population. Dyn Games Appl 2021;11(4):803–34. http://dx.doi.org/10.1007/s13235-021-00383-2.
[12] Assaf M, Mobilia M, Roberts E. Cooperation dilemma in finite populations under fluctuating environments. Phys Rev Lett 2013;111:238101. http://dx.doi.org/10.1103/PhysRevLett.111.238101.
[13] Pereda M, Zurro D, Santos JI, Briz I. Godino I, Álvarez M, Caro J, et al. Emergence and evolution of cooperation under resource pressure. Sci Rep 2017;7:45574. http://dx.doi.org/10.1038/srep45574.
[14] Szolnoki A, Chen X. Environmental feedback drives cooperation in spatial social dilemmas. EPL 2017;120:58001. http://dx.doi.org/10.1209/0295-5075/120/58001.
[15] Huang J, Zhu Y, Zhao D, Xia C, Perc M. The impact of feedbacks on evolutionary game dynamics in structured populations. Chaos 2025;35(6):063134. http://dx.doi.org/10.1063/5.0278673.
[16] Potts R. Environmental hypotheses of hominin evolution. Am J Phys Anthropol 1998;107(S27):93–136. http://dx.doi.org/10.1002/(sici)1096-8644(1998)107:27+<93::aid-ajpa5>3.0.co;2-x.
[17] Potts R, Faith JT. Alternating high and low climate variability: The context of natural selection and speciation in Plio-Pleistocene hominin evolution. J Hum Evol 2015;87:5–20. http://dx.doi.org/10.1016/j.jhevol.2015.06.014.
[18] Potts R, Behrensmeyer AK, Faith JT, Tryon CA, Brooks AS, Yellen JE, et al. Environmental dynamics during the onset of the Middle Stone Age in eastern Africa. Science 2018;360(6384):86–90. http://dx.doi.org/10.1126/science.aao2200.
[19] Lupien RL, Russell JM, Subramanian A, Kinyanjui R, Beverly EJ, Uno KT, et al. Eastern African environmental variation and its role in the evolution and cultural change of Homo over the last 1 million years. J Hum Evol 2021;157:103028. http://dx.doi.org/10.1016/j.jhevol.2021.103028.
[20] Inaba M, Akiyama E. Environmental variability promotes the evolution of cooperation among geographically dispersed groups on dynamic networks. PLOS Complex Syst 2025;2(4):e0000038. http://dx.doi.org/10.1371/journal.pcsy.0000038.
[21] Dugatkin LA, Wilson DS. Rover: A strategy for exploiting cooperators in a patchy environment. Amer Nat 1991;138(3):687–701. http://dx.doi.org/10.1086/285243.
[22] Vainstein MH, Silva ATC, Arenzon JJ. Does mobility decrease cooperation? J Theoret Biol 2007;244(4):722–8. http://dx.doi.org/10.1016/j.jtbi.2006.09.012.
[23] Cong R, Wu B, Qiu Y, Wang L. Evolution of cooperation driven by reputation-based migration. PLoS One 2012;7(5):e35776. http://dx.doi.org/10.1371/journal.pone.0035776.
[24] Chen X, Szolnoki A, Perc M. Risk-driven migration and the collective-risk social dilemma. Phys Rev E 2012;86:036101. http://dx.doi.org/10.1103/PhysRevE.86.036101.
[25] He Z, Geng Y, Shen C, Shi L. Evolution of cooperation in the spatial prisoner's dilemma game with extortion strategy under win-stay-lose-move rule. Chaos Solitons Fractals 2020;141:110421. http://dx.doi.org/10.1016/j.chaos.2020.110421.
[26] Dhakal S, Chiong R, Chica M, Middleton RH. Climate change induced migration and the evolution of cooperation. Appl Math Comput 2020;377:125090. http://dx.doi.org/10.1016/j.amc.2020.125090.
[27] Ren T, Zheng J. Evolutionary dynamics in the spatial public goods game with tolerance-based expulsion and cooperation. Chaos Solitons Fractals 2021;151:111241. http://dx.doi.org/10.1016/j.chaos.2021.111241.
[28] Yang Y, Pan Q, He M. The influence of environment-based autonomous mobility on the evolution of cooperation. Chaos Solitons Fractals 2023;169:113320. http://dx.doi.org/10.1016/j.chaos.2023.113320.
[29] Zhang H. Evolution of cooperation among fairness-seeking agents in spatial public goods game. Appl Math Comput 2025;489:129183. http://dx.doi.org/10.1016/j.amc.2024.129183.
[30] Huberman BA, Glance NS. Evolutionary games and computer simulations. Proc Natl Acad Sci USA 1993;90(16):7716–8. http://dx.doi.org/10.1073/pnas.90.16.7716.
[31] Zhang G, Xiong X, Pi B, Feng M, Perc M. Spatial public goods games with queueing and reputation. Appl Math Comput 2025;505:129533. http://dx.doi.org/10.1016/j.amc.2025.129533.
[32] Schuck-Paim C, Alonso WJ, Ottoni EB. Cognition in an ever-changing world: climatic variability is associated with brain size in Neotropical parrots. Brain Behav Evol 2008;71(3):200–15. http://dx.doi.org/10.1159/000119710.
[33] Sol D, Bacher S, Reader SM, Lefebvre L. Brain size predicts the success of mammal species introduced into novel environments. Amer Nat 2008;172(S1):S63–71. http://dx.doi.org/10.1086/588304.
[34] Sol D. Revisiting the cognitive buffer hypothesis for the evolution of large brains. Biol Lett 2009;5(1):130–3. http://dx.doi.org/10.1098/rsbl.2008.0621.
[35] Boyd R, Richerson PJ. Culture and the evolution of human cooperation. Phil. Trans. R. Soc. B 2009;364(1533):3281–8. http://dx.doi.org/10.1098/rstb.2009.0134.
[36] Henrich J, Muthukrishna M. The origins and psychology of human cooperation. Annu Rev Psychol 2021;72:207–40. http://dx.doi.org/10.1146/annurev-psych-081920-042106.
[37] Melis AP, Raihani NJ. The cognitive challenges of cooperation in human and nonhuman animals. Nat Rev Psychol 2023;2(9):523–36. http://dx.doi.org/10.1038/s44159-023-00207-7.

[38] Dunbar RIM. The social brain hypothesis - thirty years on. Ann Hum Biol 2024;51(1):2359920. http://dx.doi.org/10.1080/03014460.2024.2359920.
[39] Kollock P. Social dilemmas: The anatomy of cooperation. Annu Rev Sociol 1998;24:183–214. http://dx.doi.org/10.1146/annurev.soc.24.1.183.
[40] Perc M, Gómez-Gardeñes J, Szolnoki A, Floría LM, Moreno Y. Evolutionary dynamics of group interactions on structured populations: a review. J R. Soc Interface 2013;10(80):20120997. http://dx.doi.org/10.1098/rsif.2012.0997.
[41] Turner MA, Moya C, Smaldino PE, Jones JH. The form of uncertainty affects selection for social learning. Evol Hum Sci 2023;5:e20. http://dx.doi.org/10.1017/ehs.2023.11.
[42] Ohtsuki H, Ujiyama S. Impact of social dominance on the evolution of individual learning. J Theoret Biol 2022;535:110986. http://dx.doi.org/10.1016/j.jtbi.2021.110986.
[43] Pi B, Deng L-J, Feng M, Perc M, Kurths J. Dynamic evolution of complex networks: A reinforcement learning approach applying evolutionary games to community structure. IEEE Trans Pattern Anal Mach Intell 2025;47(10):8563–82. http://dx.doi.org/10.1109/TPAMI.2025.3579895.
[44] Lee H-W, Cleveland C, Szolnoki A. When costly migration helps to improve cooperation. Chaos 2022;32(9):093103. http://dx.doi.org/10.1063/5.0100772.